

MICROSTRUCTURAL EVOLUTION OF AUSTENITIC STAINLESS STEELS IRRADIATED TO 17 DPA IN SPECTRALLY TAILORED EXPERIMENT OF THE ORR AND HFIR AT 400°C — E. Wakai (Japan Atomic Energy Research Institute), N. Hashimoto (Oak Ridge National Laboratory), T. Sawai (JAERI), J. P. Robertson and L. T. Gibson (ORNL), I. Ioka, and A. Hishinuma (JAERI)

OBJECTIVE

The purpose of this work is to summarize the microstructural evolution of six austenitic steels irradiated at 400°C to 17.3 dpa in the spectrally tailored experiments of the ORR and HFIR.

SUMMARY

The microstructural evolution of austenitic JPCA aged and solution annealed JPCA, 316R, C, K, and HP steels irradiated at 400°C in spectrally tailored experiments of the ORR and HFIR has been investigated. The helium generation rates were about 12-16 appm He/dpa on the average up to 17.3 dpa. The number densities and average diameters of dislocation loops in the steels have ranges of 3.3×10^{21} - $9.5 \times 10^{21} \text{ m}^{-3}$ and 15.2- 26.3 nm, respectively, except for HP steel for which they are $1.1 \times 10^{23} \text{ m}^{-3}$ and 8.0 nm. Precipitates are formed in all steels except for HP steel, and the number densities and average diameters have ranges of 5.2×10^{20} - $7.7 \times 10^{21} \text{ m}^{-3}$ and 3.4- 19.3 nm, respectively. In the 316R, C, and K steels, the precipitates are also formed at grain boundaries, and the mean sizes of these are about 110, 50, and 50 nm, respectively. The number densities of cavities are about $1 \times 10^{22} \text{ m}^{-3}$ in all the steels. The swelling is low in the steels which form the precipitates.

PROGRESS AND STATUS

1. Introduction

One of the favored first wall and blanket concepts for near term fusion systems such as the International Thermonuclear Experimental Reactor (ITER) is a low pressure water-cooled austenitic stainless steel structure [1]. The neutron sources with a maximum energy of 14 MeV in the D-T fusion reactor create displacement damage in the wall, and produce hydrogen and helium atoms from (n, p) and (n, α) reactions. In the absence of operating fusion reactors, the necessary irradiation experience has to be gained from a partial simulation of the fusion environment using water-cooled mixed-spectrum fission reactors. For austenitic stainless steels, it is possible to reproduce the damage rate, neutron fluence, and helium generation rate typical of the fusion environment using spectral tailoring [2-5]. Spectral tailoring involves progressively changing the ratio of thermal to fast neutron flux through the use of removable shields surrounding the experimental assembly [2]. In this way the two-step thermal neutron reaction with ^{58}Ni [6] can be manipulated so that the ratio of helium generation rate to displacement rate (He/dpa ratio) approximates that for fusion throughout the irradiation. In this study the microstructural evolution of six types of austenitic stainless steels have been examined under the controlled He/dpa ratio. This experiment is being conducted under the DOE/JAERI Collaborative Agreement.

2. Experimental Procedure

The spectrally tailored experiments were performed in two stages. The first stage of the irradiation was carried out in the Oak Ridge Research Reactor (ORR) in capsule ORR-MFE-7J [7-12]. After accumulating approximately 7.4 dpa in the ORR, the specimens were transferred to the High Flux Isotope Reactor (HFIR) in capsule HFIR-RB-400J-1 for the second stage [13-15]. In each reactor, the specimens were irradiated at 400°C.

Table 1. Damage levels, helium concentrations, and the ratios of He/dpa of type 316 and JPCA stainless steels irradiated in the spectrally tailored experiments of the ORR and HFIR

	316 (13wt%Ni)			JPCA (16wt%Ni)		
	Damage (dpa)	He (atppm)	He/dpa	Damage (dpa)	He (atppm)	He/dpa
ORR (MFE-7J)	7.4	100	14	7.4	155	21
HFIR (RB-400J-1)	9.9	100	10	9.9	125	13
ORR + HFIR	17.3	200	12	17.3	280	16

Table 2. Chemical compositions of austenitic stainless steels used in this study (wt%)

Alloy	Fe	Cr	Ni	B	C	N	P	S	Si	Ti	Mn	Nb	Mo
JPCA	Bal.	14.2	15.6	0.003	0.06	0.003 ₉	0.027	0.005	0.50	0.24	1.77	-	2.3
316R	Bal.	16.8	13.5	-	0.06	-	0.028	0.003	0.61	0.005	1.80	-	2.5
C	Bal.	15.4	15.6	-	0.02	0.001 ₈	0.017	0.007	0.51	0.25	1.56	0.0 ₈	2.4
K	Bal.	18.0	17.6	-	0.02	0.004	0.015	0.005	0.48	0.29	1.46	-	2.6
HP	Bal.	17.1	11.8	-	0.005	0.020	-	-	0.005	-	-	-	-

Temperatures were continuously measured and controlled in these experiments during irradiation. The thermal and fast ($E > 0.1$ MeV) neutron fluences in the ORR were 8.1×10^{25} and 9.5×10^{25} n/m² [13], and those of the HFIR were 4.0×10^{25} and 1.6×10^{26} n/m² [5, 7], respectively. The experiments achieved a total peak damage level of 17.3 dpa. The helium concentration generated in type 316 and JPCA stainless steel were 200 and 280 He appm, respectively, and the controlled average ratios of He/dpa were 12 and 16 appm for the 316 and JPCA, respectively, in this irradiation. The details are listed in Table 1.

Transmission electron microscopy (TEM) disks of six different austenitic stainless steels were irradiated in these capsules. The steels are the JPCA-aged, JPCA, 316R, C, K, and HP (a high-purity ternary austenite). Chemical compositions of these alloys are given in Table 1. The JPCA steel contains boron, phosphorus, and titanium. The 316R is a standard of type 316 stainless steel. The C and K stainless steels have low carbon concentration, and they are modified exploratory alloys with titanium and/or niobium. The HP steel is a standard ternary alloy with iron, chromium, and nickel contents similar to those of type 316. The JPCA, 316R, C, K, and HP alloys were solution annealed (SA), and the JPCA aged steel was aged for 1 hr at 800 °C after 20 % cold work prior to irradiation.

Microstructures of these specimens were examined using a JEM-2000FX transmission electron microscope with a LaB₆ gun operated at 200 kV. In order to evaluate defect density the foil thickness of each TEM specimen was measured by thickness fringes or by the improved CSS method [16, 17].

3. Results and Discussion

3.1 Precipitate Formation

Precipitates are formed in all the steels, except for the HP steel, and are observed as particles with a fringe contrast as seen in Figure 1. One of the micrographs is taken by a weak beam dark-field condition, and the others are taken by a bright-field, using $g=200$, as noted in the figure. The moire fringes observed in the steels are parallel type. The precipitates are identified, from the spacing of the moire fringe, as MC type for the JPCA aged and 316R steels, $M_{23}C_6$ type for JPCA-SA and C steels, and M_6C or $M_{23}C_6$ for the K steel, respectively, as summarized in Table 3. The mean sizes and number densities of the precipitates are given in Table 4. The JPCA and 316R steels have a highest and lowest number density of precipitates, respectively. The mean size of precipitates is relatively small in steels with high number density.

The precipitates are also observed at grain boundaries in the 316R, C, and K steels as shown in Figure 2. The mean sizes of grain boundary precipitates are 110, 50, and 50 nm for the three steels, respectively, and the number density of precipitates on grain boundaries in the 316R steel is lower than that of the C and K steels. In other steels, the precipitates at grain boundaries were not observed.

Although the titanium concentration of 316R steel is low, i.e., 0.005%, MC type precipitates are formed. In the previous report [5] for the specimens from this experiment examined after the ORR irradiation to 7.4 dpa, the formation of precipitates was only in the steels with titanium

Table 3. Identification of the precipitates formed in the steels irradiated at 400°C to 17.3 dpa with a helium generation rate of about 12 -16 appm He/dpa on the average throughout this experiment

	JPCA aged	JPCA SA	316R SA	C SA	K SA
Measured the spacings of the moire fringe (nm)	1.3	1.7	1.4	1.7	2.7
Precipitate type	MC	$M_{23}C_6$	MC	$M_{23}C_6$	M_6C or $M_{23}C_6$
Lattice parameter (nm)	0.41 [18]	1.06 [19]	0.41	1.06	1.11 [19] or 1.06
The corresponding plane of the precipitates	(002)	(335)	(002)	(335)	(335) or (026)
Calculated the moire spacing (nm)	1.43	1.68	1.43	1.68	2.94 or 2.64

Table 4. Mean sizes and densities of precipitates formed in six austenitic steels irradiated at 400°C to 17.3 dpa

Alloy	Type of Precipitates	Mean Size (nm)	Number Density (m^{-3})
JPCA aged	MC	11.5	1.3×10^{21}
JPCA SA	$M_{23}C_6$	3.4	7.7×10^{21}
316R SA	MC	15.1	5.2×10^{20}
C SA	$M_{23}C_6$	5.3	5.8×10^{21}
K SA	M_6C or $M_{23}C_6$	19.3	9.5×10^{20}
HP SA	-	-	-

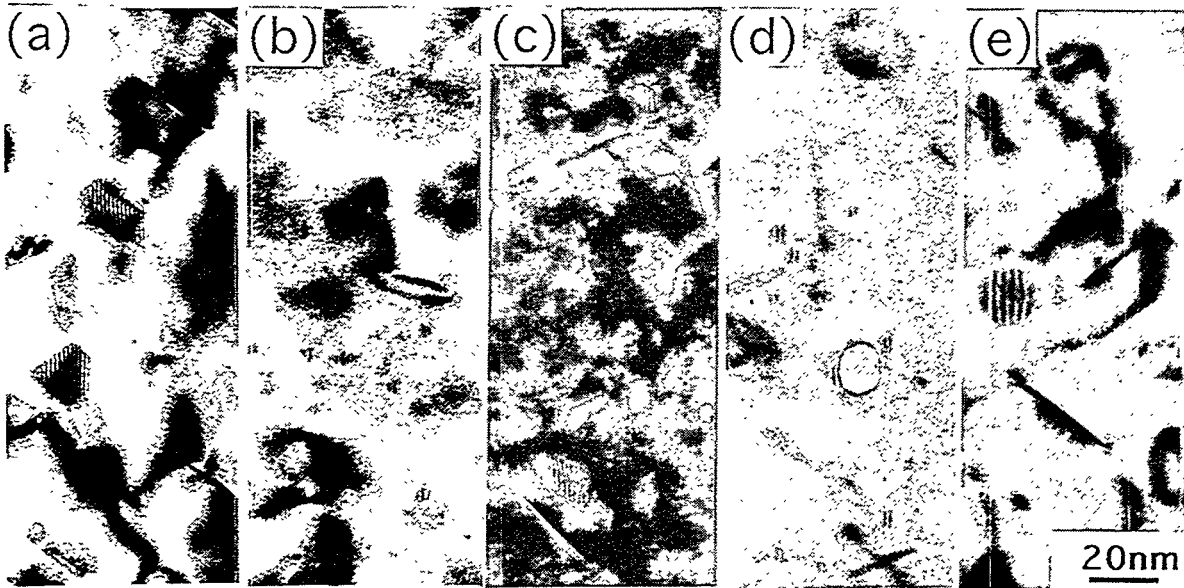


Figure 1. Precipitates formed in (a) JPCA-aged, (b) JPCA-SA, (c) 316R-SA, (d) C-SA, and (e) K-SA after irradiation at 400 °C to 17.3 dpa with a helium generation rate of about 12 -16 appm He/dpa on the average throughout this experiment. The micrographs of (a), (b), (d), and (e) are taken with bright-field image conditions, and of (c) is a weak beam dark-field condition, using $g=200$ near (011) orientation, respectively.

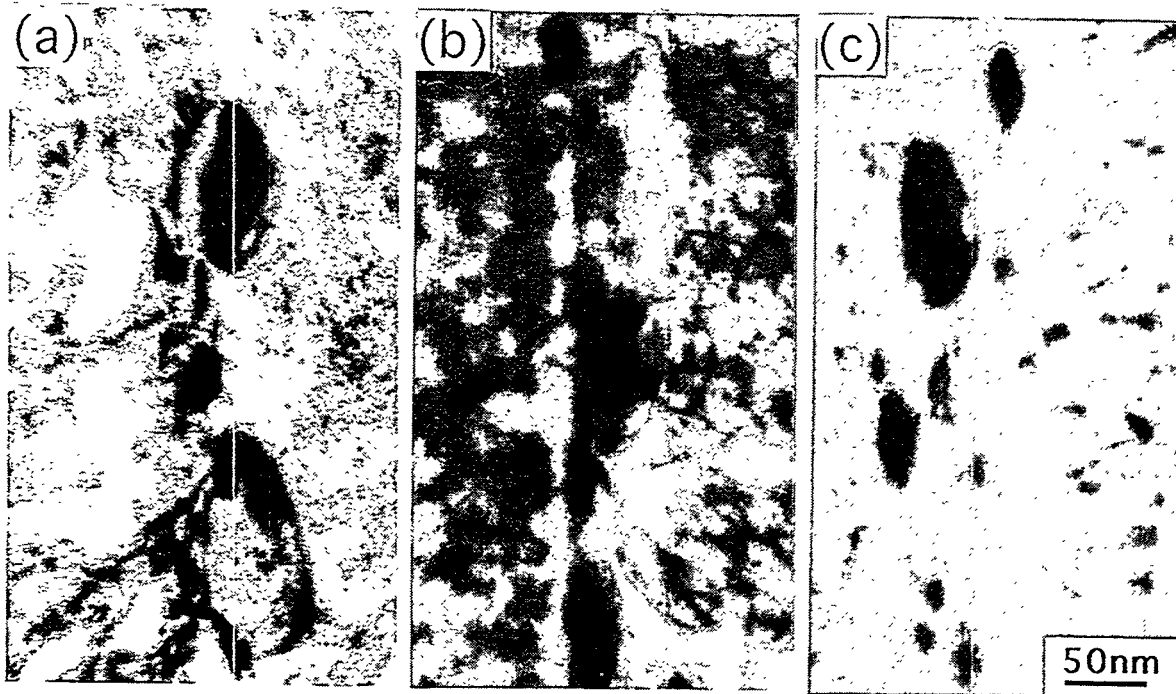


Figure 2. Precipitates at grain boundaries in (a) 316R-SA, (b) C-SA, and (c) K-SA after irradiation at 400 °C to 17.3 dpa.

Table 5. Mean sizes, number densities, and total line lengths of dislocation loops formed in six austenitic steels irradiated at 400°C to 17.3 dpa with a helium generation rate of about 12 -16 appm He/dpa on the average throughout this experiment

Alloy	Mean Size (nm)	Number Density (m ⁻³)	Total line length of the loops (m/m ³)
JPCA aged	15.2	7.3×10^{21}	3.5×10^{14}
JPCA SA	18.7	7.0×10^{21}	4.1×10^{14}
316R SA	20.2	9.5×10^{21}	6.0×10^{14}
C SA	26.3	3.3×10^{21}	2.7×10^{14}
K SA	22.1	4.5×10^{21}	3.1×10^{14}
HP SA	8.2	1.1×10^{23}	2.8×10^{15}

contents of more than 0.01 %, i.e., JPCA-SA, C, and K steels [5]. This fact appears to imply that the precipitates are still developing up to of the irradiation of 17.3 dpa. In low carbon C and K steels, the precipitates of $M_{23}C_6$ or M_6C types are formed, while in the high carbon 316R and JPCA steels the precipitates of MC or $M_{23}C_6$ are formed. Therefore, the formation of these carbides is likely intimately related with the titanium and carbon concentration.

3.2 Dislocation Loop Formation

Figure 3 shows dislocation loops formed in the six austenitic steels irradiated at 400°C to 17.3 dpa. The electron micrographs are taken with beam direction **B** close to $\langle 110 \rangle$, and are dark-field images which are formed using a streak due to stacking faults in the diffraction pattern. The loops observed are Frank loops on {111} planes in all steels, but in the K steels there are some loops which have a large size and are perfect loops; these are identified by the weak beam dark-field image. The mean sizes, number densities, and total line lengths of these loops are given in Table 5.

The mean size of the loops is the smallest in the HP steel and that of the C steel is the largest. Conversely, the number density of the loops in the HP steel is the highest and that of the C steel is the lowest. The growth of dislocation loops has a tendency to be faster in the steels with low number density of loops. The total line length of the loops is the highest in the HP. The total line lengths and the type of loops are discussed for the cavity growth in next section.

The number density of loops in HP steel is more than one order higher than those of the others as shown in Table 5. The elemental contents of the HP steel are iron, chromium, and nickel with low impurity levels as given in Table 2. However, the nitrogen concentration in the HP steel is especially higher than that of the other steels. The C steel with the lowest number density of loops contains lower carbon and nitrogen concentrations than those of the other steels. Interstitial impurities such as nitrogen and carbon may enhance the formation of dislocation loops [20]. Thus, the cause of the loop formation with a high number density may be due to be the high nitrogen concentration, and the idea is supported by the fact that the number densities of the loops in the HP and C steels are the highest and lowest, respectively.

3.3 Cavity Formation

The micrographs of cavities in the steels are as shown in Figure 4, and in the C steel the precipitates are seen on the surfaces of some cavities. The size distribution of these cavities

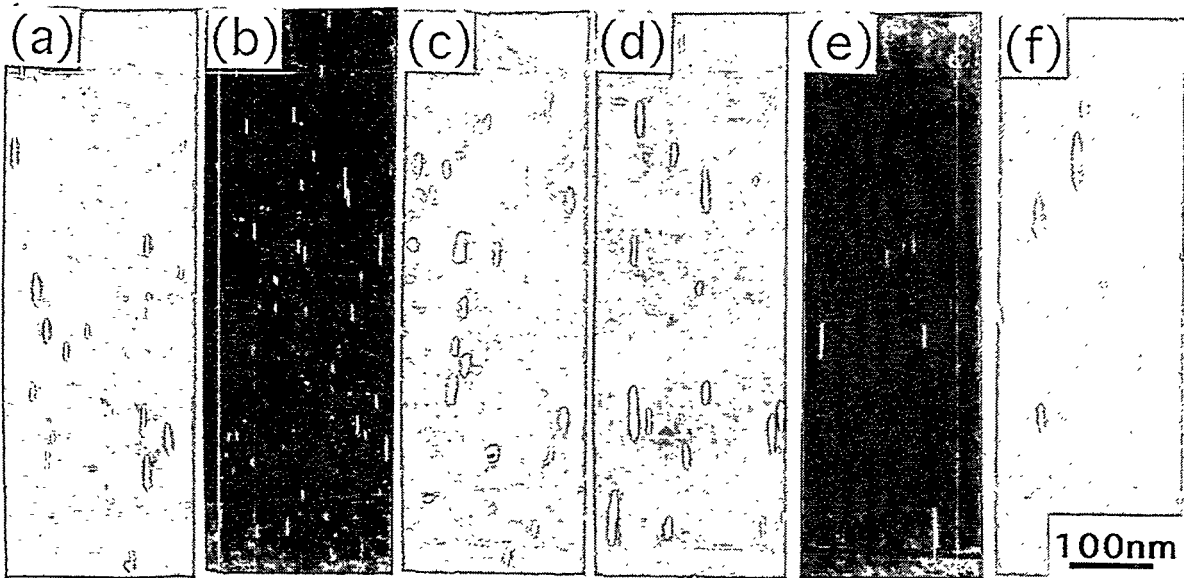


Figure 3. Dislocation loops formed in (a) JPCA -aged, (b) JPCA-SA, (c) 316R-SA, (d) C-SA, (e) K-SA, and (f) HP-SA after irradiation at 400 °C to 17.3 dpa with a helium generation rate of about 12 -16 appm He/dpa on the average throughout this experiment.

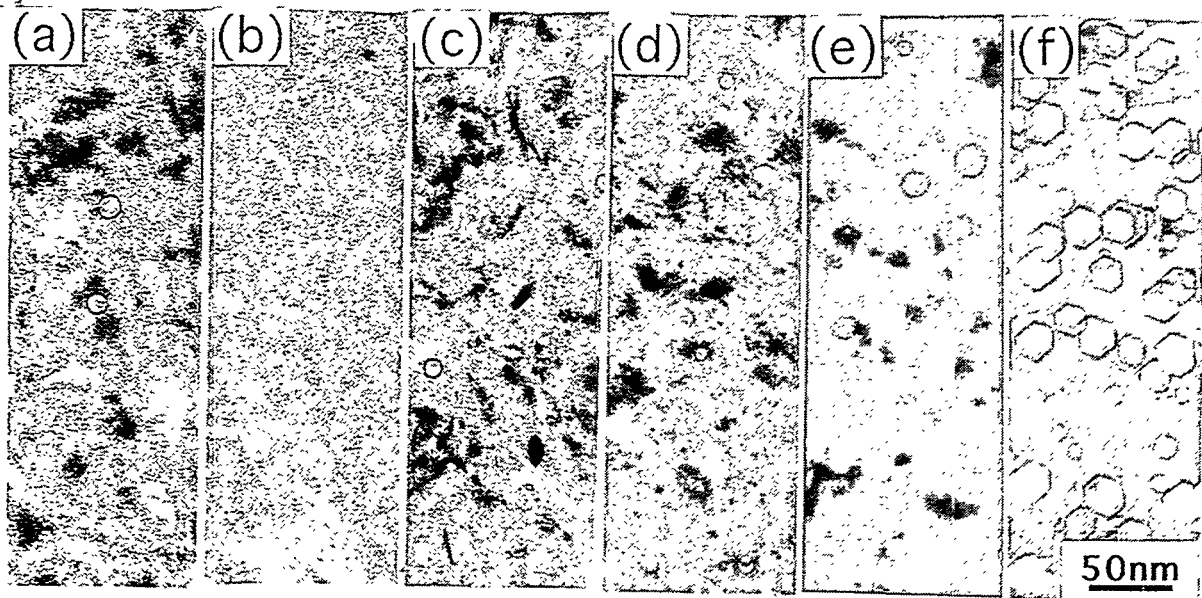


Figure 4. Cavities formed in (a) JPCA-aged, (b) JPCA-SA, (c) 316R-SA, (d) C-SA, (e) K-SA, and (f) HP-SA after irradiation at 400 °C to 17.3 dpa with a helium generation rate of about 12 -16 appm He/dpa on the average throughout this experiment.

Table 6. Swelling data of the cavities formed in six austenitic steels irradiated at 400°C to 17.3 dpa with a helium generation rate of about 12 -16 appm He/dpa on the average throughout this experiment

Alloy	Root Mean Cube of Cavity Radius (nm)	Number Density (m ⁻³)	Swelling (%)
JPCA aged	1.4	1.7 x 10 ²²	0.020
JPCA SA	1.5	1.1 x 10 ²²	0.016
316R SA	1.8	6.2 x 10 ²¹	0.015
C SA	2.5	1.1 x 10 ²²	0.079
K SA	4.0	1.0 x 10 ²²	0.27
HP SA	7.2	1.9 x 10 ²²	2.9

is given in Figure 5, and the distributions of cavities are bi-modal. The swelling, S, is described as:

$$S = (V/V) \times 100 (\%) = (400\pi/3) R_r^3 \times N,$$

where V' is total volume of all cavities per unit volume, V; N is a total number of cavities per unit volume; and R_r is the root mean cube of cavity radius (RMC radius).

The RMC radius is described as;

$$R_r = (\sum R_i^3 / N)^{1/3},$$

where R_i is a cavity radius i. The RMC radius, number density, and swelling are summarized in Table 6 for each steel.

In HP steel the RMC radius is the largest and the number density is also the highest of all steels, and therefore the value of swelling is the highest. The number densities of the cavities are about 1 x 10²² m⁻³ in all the steels. However, the swelling has a large alloy dependence, i.e., except for the K and HP steels the swelling is very low. In this experiment, the steels which formed the precipitates have relatively low swelling values.

In this experiment the HP steel has no precipitate formation and a high number density of the loops, while the other steels have many precipitates and relatively low number density of the loops. Thus, there appears to be a relationship between the precipitate development and cavity growth. The cause of cavity growth suppression in steels which form the precipitates is thought to be due to two effects. One is the decrease of vacancy oversaturation concentration due to dislocations with shorter total line lengths [21, 22] as given in Table 5. Another is the increase of recombination for vacancy and interstitial atoms at the precipitates, which are in high density. Therefore, the vacancy concentration in the other steels under irradiation may be lower than that of the HP steels, leading to a high swelling value.

The K steel has a relatively large swelling, but the line length of the loops of K steel is nearly the same as those of the other steels which form the precipitates as given in Tables 5 and 6. The K steel has not only Frank loops but also perfect loops, which have a strong bias factor [21, 22], compared with that of the Frank loops. Therefore, the larger swelling of the K steel may be due to a strong bias factor of the perfect loops.

Finally, the comparison of the reference data [23, 24] for the non-spectrally tailored experiments (non-ST experiments) of the HFIR irradiation and the present data of the spectrally tailored one for the same steels is listed in Table 7. The number densities of dislocation loops of the non-ST ones are higher than those of the present work, and the total

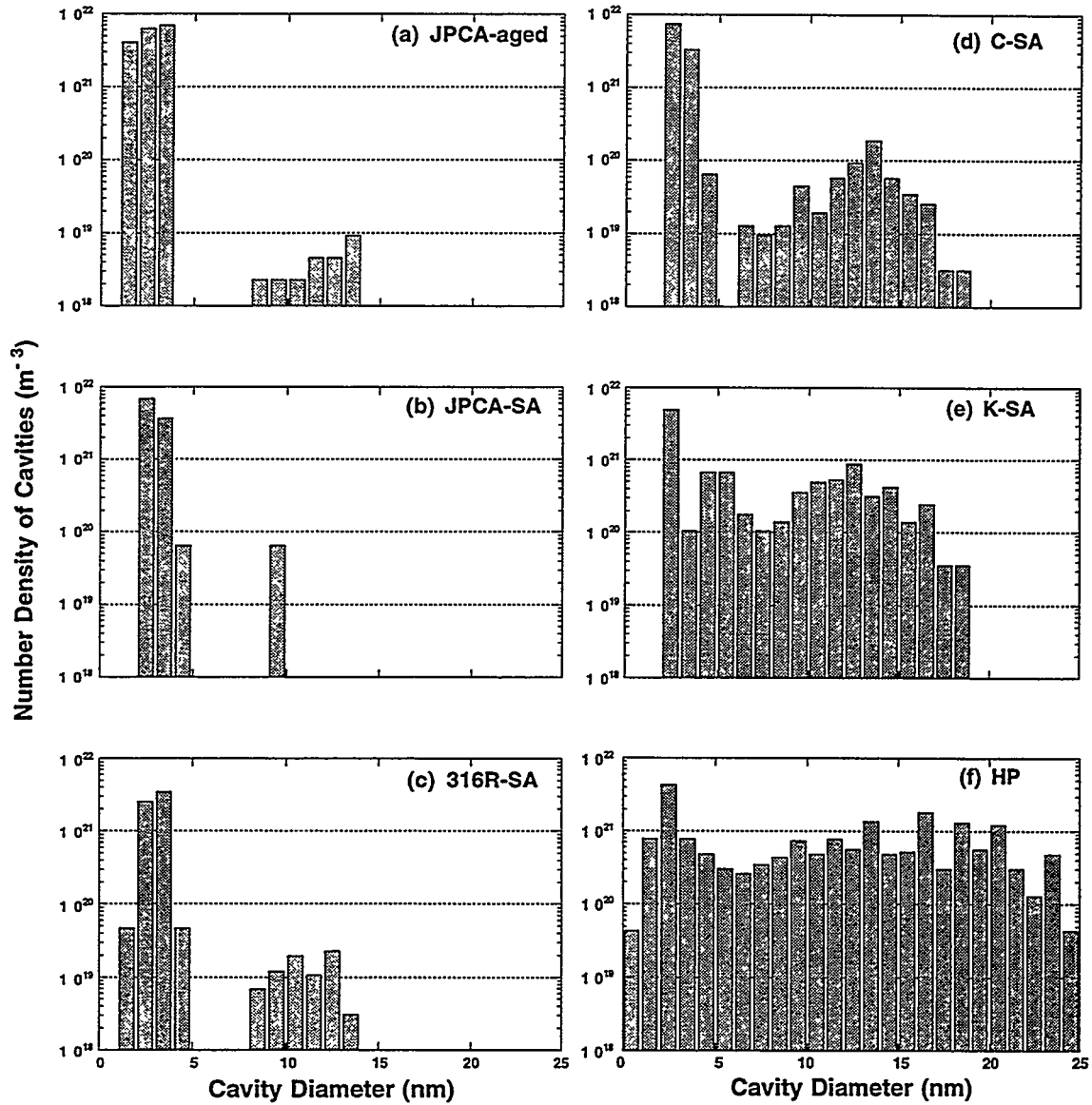


Figure 5 Size distribution of cavities in (a) JPCA-aged, (b) JPCA-SA, (c) 316R-SA, (d) C-SA, (e) K-SA, and (f) HP after irradiation at 400 °C to 17.3 dpa.

Table. 7. Comparison of the reference data of the non-spectrally tailored experiments (non-ST) of the HFIR irradiation [21, 22] and this spectrally tailored one (ST) for the same steels

	Irradiations			Cavities			Loops			Precipitates	
	Temp. (°C)	Damage (dpa)	He (atppm)	Mean size (nm)	Number density (m ⁻³)	Swelling (%)	Mean size (nm)	Number density (m ⁻³)	Total line length (m/m ³)	Mean size (nm)	Number density (m ⁻³)
Reference data (non-ST)											
JPCA-SA	400	10.2	530	1.8	2.9x10 ²³	0.08	12.0	2.0x10 ²²	7.5x10 ¹⁴	0	0
JPCA-SA	400	33.6	2470	2.6	2.9x10 ²³	0.25	12.3	2.4x10 ²²	9.3x10 ¹⁴	3.1	1.9x10 ²²
316R-SA	400	33.4	2140	2.3	3.4x10 ²²	0.22	16.0	2.5x10 ²²	1.3x10 ¹⁵	-	-
Present data (ST)											
JPCA-SA	400	17.3	280	1.5	1.1x10 ²²	0.016	18.7	7.0x10 ²¹	4.1x10 ¹⁴	3.4	7.7x10 ²¹
316R-SA	400	17.3	200	1.8	6.2x10 ²¹	0.015	20.2	9.5x10 ²¹	6.0x10 ¹⁴	15.1	5.2x10 ²⁰

line length of the loops is longer. In the non ST experiments, the helium generation, the mean size, number density, and the swelling of the cavities are higher than those of the present work.

FUTURE WORK

Comparisons of these data with those from the first stage of the experiment (7.4 dpa in the ORR) as well as the microstructural analyses of cold worked specimens in the HFIR-400J-1 capsule are still in progress. Void swelling measurement by immersion densitometry will be also performed for the same specimens.

ACKNOWLEDGMENTS

The authors are grateful to Messrs. A. T. Fisher, J. W. Jones, J. J. Duff, and members of hot laboratory of ORNL for the technical support.

REFERENCES

1. G. L. Kulcinski, J. Nucl. Mater., **122&123**(1984)457.
2. M. L. Grossbeck et al., in: Proc. Conf. on Fast, Thermal, and Fusion Reactor Experiments, Salt Lake City, Utah, April 1985, Vol. 1, pp. 199-210.
3. A. F. Rowcliffe, A. Hishinuma, M. L. Grossbeck, and S. Jitsukawa, J. Nucl. Mater., **179-181** (1991)125.
4. R. E. Stoller, P. J. Maziasz, A. F. Rowcliffe, and M. P. Tanaka, J. Nucl. Mater., **155-157** (1988)1328.
5. T. Sawai, P. J. Maziasz, H. Kanazawa, and A. Hishinuma, J. Nucl. Mater., **191-194** (1992) 712.
6. A. A. Bauer and M. Kangilaski, J. Nucl. Mater., **42**(1972)91.
7. J. P. Robertson, I. Ioka, A. F. Rowcliffe, M. L. Grossbeck, and S. Jitsukawa, Effects of Radiation on Materials: 18th International Symposium, ASTM STP 1325, R. K. Nastad, et al., Eds., American Society for Testing and Materials, Philadelphia, 1997.
8. I. I. Siman-Tov, Fusion Reactor Materials Semiannual Progress Report for Period Ending September 30, 1987, Office of Fusion Energy, DOE/ER-0313/3, 1988, p. 7.
9. L. R. Greenwood, Fusion Reactor Materials Semiannual Progress Report for Period Ending March 31, 1989, Office of Fusion Energy, DOE/ER-0313/6, 1989, p. 23.

10. L. R. Greenwood and D. V. Steidl, Fusion Reactor Materials Semiannual Progress Report for Period Ending March 31, 1990, Office of Fusion Energy, DOE/ER-0313/8, 1990, p. 34.
11. L. R. Greenwood, Alloy Development for Irradiation Performance Semiannual Progress Report for Period Ending March 31, 1989, Office of Fusion Energy, DOE/ER-0045/16, 1986, p. 17.
12. T. Sawai, P. J. Maziasz, H. Kanazawa and A. Hishinuma, Fusion Reactor Materials Semiannual Progress Report for Period Ending September 30, 1990, Office of Fusion Energy, DOE/ER-0313/9, 1990, p. 152.
13. L. R. Greenwood, C. A. Baldwin and B. M. Oliver, Fusion Reactor Materials Semiannual Progress Report for Period Ending September 30, 1994, Office of Fusion Energy, DOE/ER-0313/17, 1995, p. 28.
14. A. W. Longest, J. E. Pawel, D. W. Heatherly, R. G. Sitterson, and R. L. Wallace, Fusion Reactor Materials Semiannual Progress Report for Period Ending March 31, 1993, Office of Fusion Energy, DOE/ER-0313/14, 1993, p. 14.
15. A. W. Longest, D. W. Heatherly, E. D. Clemmer, and J. E. Corum, Fusion Reactor Materials Semiannual Progress Report for Period Ending March 31, 1993, Office of Fusion Energy, DOE/ER-0313/14, 1993, p. 14.
16. T. Sawai, M. Suzuki, P. J. Maziasz, and A. Hishinuma, *J. Nucl. Mater.*, **187**(1992)146.
17. T. Sawai, and M. Suzuki, *Scripta Metall.*, **24**(1990)2047.
18. E. H. Lee, P. J. Maziasz, and A. F. Rowcliffe, in: *Phase Stability During Irradiation*, Eds. J. R. Holland, L. K. Mansur, and D. I. Potter (TMS-AIME, Warrendale, PA, 1981)pp. 191-218.
19. K. W. Andrews, D. J. Dyson, and S. R. Keown, in: *Interpretation of Electron Diffraction Patterns* (Plenum Press, New York), p172.
20. E. Wakai, A. Hishinuma, Y. Kato, S. Takaki, and K. Abiko, *Proc. Ultra High Purity Base Metals*, Ed. K. Abiko, K. Hirakawa, and S. Takaki, The Japan Institute of Metals, Sendai (Japan) 1994 p. 522.
21. W. G. Wolfer and M. Ashkin, *J. Applied Phys.*, **47**(1976)791.
22. W. G. Wolfer, L. K. Mansur, and J. A. Sprague, *Proc. Intern. Conf. on Radiation Effects in Breeder Reactor Structural Materials*. Scottsdale, Az (1977) eds. M. L. Bleiberg and J. W. Bennett, p. 841.
23. M. P. Tanaka, P. J. Maziasz, A. Hishinuma, and S. Hamada, *J. Nucl. Mater.*, **141-143** (1986) 943.
24. S. Hamada, P. J. Maziasz, M. P. Tanaka, M. Suzuki, and A. Hishinuma, *J. Nucl. Mater.*, **155- 157** (1988) 838.